Title of paper:

Local Plastic Mechanisms in Thin Steel Plates under In-plane Compression

Abstract

Thin-walled steel plates subjected to in-plane compression develop two types of local plastic mechanism, namely the roof-shaped mechanism and the so-called flip-disc mechanism, but the intriguing question of why two mechanisms should develop was not answered until recently. It was considered that the location of first yield point shifted from the centre of the plate to the midpoint of the longitudinal edge depending on the b/t ratio, imperfection level, and yield stress of steel, which then decided the type of mechanism. This paper has verified this hypothesis using analysis and laboratory experiments. An elastic analysis using Galerkin's method to solve Marguerre's equations was first used to determine the first yield point, based on which the local plastic mechanism / imperfection tolerance tables have been developed which give the type of mechanism as a function of b/t ratio, imperfection level and yield stress of steel. Laboratory experiments of thin-walled columns verified the imperfection tolerance tables and thus indirectly the hypothesis. Elastic and rigid-plastic curves were then used to predict the effect on the ultimate load due to the change of mechanism. A finite element analysis of selected cases also confirmed the results from simple analyses and experiments.

1. Introduction

Thin-walled steel structures are widely used in the building and construction industry because of their high strength and light weight attributes. Their use has expanded rapidly in recent times with the introduction of thinner and higher strength steels. Thin-walled steel structures often develop local buckling and local plastic mechanisms, both of which are essential features determining their behaviour. The rigid-plastic curve based on the observed local plastic mechanism, and the elastic curve could be developed from simple analyses, and they can be used to draw the framework around the actual behaviour of thin-walled structures. The intersection of elastic and rigid-plastic curves can be used to estimate the ultimate load. Murray and his co-workers have often used this approach in their research work on thin-walled steel structures under various loadings[1].

Michelutti's[2] tests on stiffened steel plates under axial compressive and transverse loading showed a sudden drop in ultimate load when the type of mechanism switched from one to another. When thin steel plates are loaded with in-plane compression, similar behaviour can be anticipated because two types of local plastic mechanisms, namely the roof-shaped mechanism and the so-called flip-disc mechanism, are observed (see Figure 1).

Flip-disc mechanisms were observed on plates having a large plate slenderness ratio b/t (or width to thickness ratio), and roof-shaped mechanisms on plates having a smaller b/t ratio. The intriguing question of why two mechanisms should have developed remained unanswered until recently. Murray[3] postulated that the location of first yield point shifted from the centre of the plate to the midpoint of the longitudinal edge as the b/t ratio increased. Once yielding has commenced either at the centre or at the edge of the plate, the plastic mechanism was attached to these points and grew outwards from them, and thus decided the type of mechanism. The location of the first yield point is influenced by the magnitude of initial imperfections because there have been instances when mild steel plates (Grade 250 steel) of moderate b/t ratios (say 70) develop both types of mechanisms depending on the magnitude of

initial imperfections. Obviously the type of mechanism will also depend on the yield stress of steel in addition to the b/t ratio and initial imperfections. Determining the effects of these three parameters on the formation of local plastic mechanisms and the point at which they cause a transition in mechanism type are of particular importance to the researchers and designers of thin-walled steel structures, particularly because such transition may be associated with a reduction in ultimate strength of such plate assemblies.

In order to investigate the change of mechanism in imperfect plates with varying b/t ratio and yield stress and to validate Murray's[3] hypothesis in relation to the formation of mechanisms, an analytical study using Galerkin's method of solving Marguerre's equations was carried out. The elastic curve thus derived together with the appropriate rigid-plastic curve obtained for the respective plastic mechanism were used to study the overall behaviour of imperfect plates including the prediction of the ultimate load. Laboratory experiments on thin steel box and C-columns of different b/t ratios and yield stress were also conducted to verify the analytical predictions. Selected cases were also investigated using a finite element analysis. This paper presents the details of these analytical and experimental studies and their results.

2. Analysis of Imperfect Plates under In-plane Compression

2.1 Second Order Elastic Analysis

Marguerre's simultaneous non-linear partial differential equations (Equation (1)) can be used to study the elastic behaviour of a geometrically imperfect isotropic plate with in-plane compression shown in Figure 2.

$$\nabla^4\phi + Et\,(y''\,w\cdot\cdot - 2y'\cdot\,w'\cdot + y\cdot\cdot\,w'' + w''\,w\cdot\cdot - w'\cdot^2) = 0 \qquad (1a)$$

$$D\,\nabla^4 w - [\phi\cdot\cdot\,(y+w)'' - 2\phi'\cdot\,(y+w)'\cdot + \phi''\,(y+w)\cdot\cdot] = 0 \qquad (1b)$$

where ' and · refer to differentiation with respect to z and x, respectively,

y is the initial geometric imperfection of plate

w is the additional out of plane deflection, and

ϕ is a stress function.

These simultaneous equations can be solved by a number of methods such as the finite difference method, the Galerkin's method, the iterative numerical methods and the perturbation technique in order to study the elastic buckling and post-buckling behaviour of plates[1]. The purpose of this analysis is to determine the stress distributions and the central out-of-plane deflections for plates of different b/t ratios with varying magnitude of initial imperfections under axial compression. An approximate solution obtained by means of Galerkin's method was used for this purpose. Murray[1] gives the details of this method and the general results of such an analysis for an imperfect plate under three different, but common simply supported boundary conditions along the longitudinal edges. In the analysis, Murray[1] assumed the following equations for the out-of-plane deflection w and the initial geometric imperfection of plate y.

$$w = w_0 \cos \beta x \cos \lambda z \qquad (2)$$

$$y = y_0 \cos \beta x \cos \lambda z \qquad (3)$$

where $\beta = \pi/b$, $\lambda = \pi/L$

w_0 = maximum out-of-plane deflection and

y_0 = maximum initial imperfection of plate

For the present study, a square plate of width b (L = b in Figure 2) and thickness t under axial compression with longitudinal edge boundary conditions as in a square column or a narrow stiffened plate is considered (Case C, Murray[1]). In this case the membrane stresses σ_z , σ_x , and τ_{xz} are given by the following Equations 4(a) to (c).

$$\frac{\sigma_z}{E} = [4C_1\lambda^2 \cosh 2\lambda x + C_2(4\lambda^2 x \sinh 2\lambda x + 4\lambda \cosh 2\lambda x)]\cos 2\lambda z + w_0(w_0 + 2y_0)\frac{\lambda^2}{8}\cos 2\beta x + p \quad (4a)$$

$$\frac{\sigma_x}{E} = -4\lambda^2(C_1 \cosh 2\lambda x + C_2 x \sinh 2\lambda x)\cos 2\lambda z + w_0(w_0 + 2y_0)\frac{\beta^2}{8}\cos 2\lambda z \quad (4b)$$

$$\frac{\tau_{xz}}{E} = 2\lambda[2\lambda C_1 \sinh 2\lambda x + C_2(2\lambda x \cosh 2\lambda x + \sinh 2\lambda x)]\sin 2\lambda z \quad (4c)$$

where **p, the average axial compressive stress in z direction**/E is given by the following.

$$\frac{b^2}{32}[2p(w_0 + y_0)\lambda^2 + 2\frac{Dw_0}{Et}(\lambda^2 + \beta^2)^2 + \frac{1}{8}w_0(w_0 + y_0)(w_0 + 2y_0)(\lambda^4 + \beta^4)] =$$
$$\frac{1}{8}b\beta^2 C_1\lambda(w_0 + y_0)\sinh\lambda b + \frac{1}{8}b\lambda^2 C_2(w_0 + y_0)(\beta^2 - \lambda^2).[\frac{\lambda b}{2}(\frac{1}{\lambda^2} - \frac{1}{\lambda^2 + \beta^2})\cosh\lambda b +$$
$$\frac{1}{2}\{\frac{\lambda^2 - \beta^2}{(\lambda^2 + \beta^2)^2} - \frac{1}{\lambda^2}\}\sinh\lambda b] + \frac{bC_2\lambda^3\beta}{4(\lambda^2 + \beta^2)}(w_0 + y_0)(\frac{\beta b}{2}\cosh\lambda b - \frac{\beta\lambda}{\lambda^2 + \beta^2}\sinh\beta b)$$

$$C_1 = \frac{-\beta^2(b\coth\lambda b + \frac{1}{\lambda})}{32\lambda^2(b\sinh\lambda b - b\cosh\lambda b.\coth\lambda b - \frac{1}{\lambda}\cosh\lambda b)}\ w_0\ (w_0 + 2y_0)$$

$$C_2 = \frac{\beta^2}{16\lambda^2(b\sinh\lambda b - b\cosh\lambda b.\coth\lambda b - \frac{1}{\lambda}\cosh\lambda b)}\ w_0\ (w_0 + 2y_0)$$

D = Plate stiffness $\frac{Et^3}{12(1-\mu^2)}$

E = Young's Modulus and μ = Poisson's ratio

In using Equation (4) for a plate of given dimensions (b x b), the maximum initial geometric imperfection (y_0) and additional central deflection (w_0) were assumed. The average stress parameter p was evaluated first and then the membrane stresses. Typical results obtained for plates with different magnitudes of initial imperfections, and with different geometry (b/L) and boundary conditions are presented in Murray[1]. The accuracy of Equation (4) is verified by the fact that p from the equation gives the elastic buckling stress for perfect plates (zero level of initial imperfection y_0).

For a perfect plate, the membrane stress σ_z remains uniformly distributed until the plate reaches its buckling stress σ_{cr} beyond which the edges carry a higher compressive stress than the middle part of the plate. In contrast, the edges of an imperfect plate have to carry a higher membrane stress from the beginning of the loading itself. With increasing load and out-of-plane deflections, the membrane stress in the middle of the plate may even become tensile.

The growth of out-of-pane deflection causes the bending stress in the middle of the plate to increase rapidly, but the bending stresses along the edges are zero since the edges remain straight. The maximum bending stresses in both z and x directions are given by Equations (5a) and (5b).

$$\sigma_{zmax} = \pm \frac{E w_0 t(\lambda^2 + \mu\beta^2)}{2(1-\mu^2)} \cos\lambda z \cos\beta x \qquad (5a)$$

$$\sigma_{xmax} = \pm \frac{E w_0 t(\beta^2 + \mu\lambda^2)}{2(1-\mu^2)} \cos\lambda z \cos\beta x \qquad (5b)$$

where μ is the Poisson's ratio.

The overall stresses in the plate were obtained by summing algebraically Equations (4) and (5). The material properties, Young's modulus (E) and Poisson's ratio (μ) were assumed to be equal to 200 GPa and 0.3, respectively for all grades of steel. In this analysis it was required to find the point of first yield in an imperfect plate when its b/t ratio and the level of initial

imperfections are varied for each grade of steel. The point of first yield is not obvious due to the presence of bending stresses and non-uniform membrane stresses. However, it is usually either at the centre of the plate or at the midpoint of the longitudinal edge. It is assumed that yielding occurs when the equivalent stress according to the von Mises yield criterion reaches the material tensile yield stress. Depending on the b/t ratio, the magnitude of initial imperfections and the yield stress of steel, yielding begins at one of the points mentioned above.

As a first step the analysis described above produced the information regarding the location of first yield point, that is, the centre of the plate or the midpoint of the longitudinal edge, for plates of particular yield stress as a function of b/t ratio and magnitude of initial geometric imperfections y_0/t. This was then used to assign the type of mechanism in each case using Murray's[3] hypothesis, that is, if the first yield point is at the centre of the plate, then a roof type mechanism will develop whereas a flip-disc type mechanism will develop when it is at the midpoint of the longitudinal edge. This resulted in local plastic mechanism tables for yield stress of steel varying from 250 MPa to 650 MPa in steps of 50 MPa. These tables thus cover all the steel grades, b/t ratios and imperfections commonly encountered in the building and construction industry. However, only two of these tables for 250 and 650 MPa are presented here as Tables 1 (a) and (b). Other tables can be found in Bernard[4].

Tables 1(a) and (b) indicate the change of mechanism when the plate gets thinner (increasing b/t ratio) or when the magnitude of maximum initial geometric imperfection (y_0/t) increases. As seen in Table 1(a), mild steel plates (250 MPa) of b/t ratio of 100 and above always form flip-disc mechanisms, however, plates with a b/t ratio less than 100 can develop either mechanism depending on y_0/t. There is a critical magnitude of initial imperfection for each b/t ratio at which the mechanism changes (see Tables 1(a) and (b)). This critical value increases with decreasing b/t ratio. Thicker plates (say b/t ratio of 20 to 40) usually do not have higher level of initial imperfections, and thus they would develop roof mechanisms. However, plates with moderate b/t ratios would develop either of the mechanism depending

on the magnitude of initial imperfection. For example a plate with a b/t ratio of 60 can develop a roof mechanism if y_0/t is less than 0.4 and a flip-disc mechanism if y_0/t is greater than 0.5 (see Table 1 (a)).

With increasing yield stress of steel, it is seen that a flip-disc mechanism could develop for smaller b/t ratios. For example, even thicker steel plates with a b/t ratio of 60 are likely to develop flip-disc mechanisms when the steel yield stress is 650 MPa (see Table 1(b)). Results also indicate that the level of initial imperfections required to change the mechanism type from roof to flip-disc is lower as the b/t ratio increases for all steel grades. This suggests that the initial imperfection level is more critical for slender plates.

As it may be desirable to avoid change of mechanism and the associated reduction in ultimate strength in thin plated structures, Tables 1(a) and (b) and others derived in this investigation[4] can be used as imperfection tolerance tables in their design and manufacturing. It is to be noted that in this analysis only the effect of geometric imperfections y_0/t was considered. The effect of residual stresses was not included, but this problem may be overcome by using y_0/t as an equivalent imperfection parameter including both geometric and residual stress-caused imperfections. It is also important to note that results are applicable to plates with simply supported longitudinal edges as in a square box-column or a narrow stiffened plate (Case C, Murray[1]).

Results for all grades of steel can be presented in a single table or by an equation if the plate slenderness b/t can be modified to $S = \frac{b}{t}\sqrt{\frac{\sigma_f}{E}}$ so that it includes the yield stress of steel σ_f. For this purpose, the b/t values of tables developed[4] for each yield stress from 250 to 650 MPa at intervals of 50 MPa were converted to the above form by using the relevant σ_f values and an E value of 200,000 MPa. Based on these results, a critical value of S at which a change of mechanism occurred was determined for each initial imperfection value y_0/t. This led to the

following equation relating y_0/t and S. Figure 3 shows the significance of this equation in a graphical format.

$$y_0/t = 0.67 + 0.086\ S - 0.081\ S^2 \qquad (6)$$

2.2 Rigid-Plastic Analysis

Murray[1] presents the basic rigid-plastic theory applied to thin-walled structures. In this analysis of roof and flip-disc mechanisms observed with plates under axial compression, rigid-plastic curves derived by Mahendran[5] and Mahendran and Murray[6] were used. In their analyses, the idealised roof mechanism was considered in two parts, the inner region of width b-2c and the two identical edge region each of width c (see Figure 1). Equilibrium of a strip element for each region was considered using a small deflection theory to derive Equation (7) for the average axial stress σ. The basic geometric parameters α, c and r in Equation (7) were assumed to be 30°, 0.2 b and 0.6, respectively, to obtain the rigid-plastic curve shown in Figure 4.

$$\frac{\sigma}{\sigma_f} = \frac{b-2c}{b}\left[\sqrt{(1+r)^2\left(\frac{\Delta}{t}\right)^2+1} - (1+r)\frac{\Delta}{t}\right] + \frac{c}{b}\left[\sqrt{\Delta_{kt}{}^2+1} - \Delta_{kt} + \frac{1}{\Delta_{kt}}\ln\left(\Delta_{kt}+\sqrt{\Delta_{kt}{}^2+1}\right)\right]$$

where $\Delta_{kt} = \dfrac{2(1+r)}{(k_1+k_2)}\ \dfrac{\Delta}{t}$ (7)

$k_1 = \text{cosec}^2\,\alpha$, $k_2 = \text{cosec}^2\,\gamma$ and

σ_f is the yield stress

$$\frac{\sigma}{\sigma_f} = \frac{1}{6}\left[1 - 2\frac{\Delta}{t} + \sqrt{\left(\frac{2\Delta}{t}\right)^2+1} - \frac{6\frac{\Delta}{t}}{\left(1+4\frac{a^2}{b^2}\right)} + 4\sqrt{\left\{\frac{3\frac{\Delta}{t}}{2\left(1+4\frac{a^2}{b^2}\right)}\right\}^2+1}\ \right] \qquad (8)$$

For the idealised flip-disc mechanism (parabolic shape, see Figure 1), the average axial stress was obtained approximately using Simpson's rule[1]. Equilibrium of a strip element was considered using a small deflection theory to derive Equation (8). It is noted that this equation is approximate because of the fairly coarse application of Simpson's rule. Accuracy of the solution is improved by using more integration points[5]. Hence this procedure was adopted in deriving the rigid-plastic curve shown in Figure 4 for the basic geometric parameter a of 0.2 b.

2.3 Ultimate Strength of Imperfect Plates

The intersection of the elastic curve (Section 2.1) and the rigid-plastic curve (Section 2.2) derived in the earlier sections can now be used to estimate the ultimate strength of plates of varying b/t ratios and imperfections. As seen in Tables 1 (a) and (b), for each b/t ratio, there is a critical initial imperfection level beyond which the type of mechanism changes from roof type to flip-disc type. It is anticipated that there could be a sudden change in the ultimate load because the imperfection level has caused a change of mechanism.

In order to verify this, a mild steel plate (yield stress of 250 MPa) with a moderate b/t ratio of 60 was considered. Figure 4 presents the elastic curves for two initial imperfection levels (y_0/t) selected on either side of the critical level, and the rigid-plastic curves for both flip-disc and roof type mechanisms. Since the type of mechanism changes from roof type to flip-disc type when y_0/t increases from 0.4 to 0.5, the ultimate strength will decrease from 0.53 (expressed as a ratio of the material yield stress) to 0.44 (see Figure 4). The ultimate strength will be 0.50 if the roof mechanism develops in both cases. Thus a reduction of about 15% is predicted in this case as a result of the change of mechanism. This reduction is not as severe as that observed in the case of Michelutti's[2] tests on stiffened plates where the mechanism actually switched from the plate to the stiffeners. However, both observations highlight the

possible reduction in the ultimate strength of a thin-walled structure when the type of local plastic mechanism changes.

3. Experimental Analysis

In order to verify the local plastic mechanism tables and in turn to verify Murray's[3] hypothesis, a total of 40 square box and lipped C-columns with varying b/t ratio and yield stress of steel were tested under axial compression. The C-columns were made by cold-bending to the required sizes whereas the square box-columns were made by welding either two angles or two C-sections. Attempts were made to minimise the initial imperfection levels in the test specimens by taking special care during fabrication of specimens. This appeared to have introduced only smaller initial geometrical imperfections, however, residual stresses in box-specimens due to even lighter welding could not be avoided. Figure 5 shows the testing of these columns in the Tinius-Olsen Testing machine in the structures laboratory. Axial shortening of the column and out-of-plane deflection of plate elements were measured (see Figure 5) during the experiments which were continued past the maximum load into the collapse region.

The typical roof and flip-disc type mechanisms observed on the lipped C- and Box-specimens are shown in Figure 6. Tables 2 (a) and (b) present the local plastic mechanism results from these experiments on lipped C-specimens and square box-specimens, respectively. Analytical predictions for zero initial imperfections from Tables 1 (a) and (b) and others developed in this investigation are compared with these experimental results assuming that test specimens had negligible imperfections. Experimental buckling and ultimate loads for these specimens are given in Bernard[4].

Approximately 80% of the experimental results agreed with the analytical predictions as seen in Tables 2 (a) and (b). In most of the other cases, a flip-disc mechanism was observed instead of a roof mechanism due to greater imperfections in the specimens. Furthermore,

these cases were located near the critical b/t ratio and hence either mechanism could have resulted depending on the level of imperfections. Box-specimens fabricated by welding together two C-sections may have resulted in higher residual stress and geometric imperfections. This may have caused the formation of flip-disc mechanisms in those box-specimens where analysis predicted roof mechanisms.

The overall conclusion from this investigation is that experiments verified the analytical predictions regarding the local plastic mechanisms for different grade steels and b/t ratios. Differences were observed only in the cases of critical transition b/t ratio and high imperfections. Therefore Tables 1 (a) and (b) and others developed in this investigation[4] or Equation (6) can be used satisfactorily to predict the type of mechanism in thin steel plates considered in this investigation. These observations also validate Murray's[3] hypothesis that the type of mechanism depends on the location of first yield point. Although the analysis did not include the effect of residual stresses, results can still be used provided an equivalent geometric imperfection can be determined.

4. Finite Element Analysis of Imperfect Plates

An investigation using an available finite element program NASTRAN[7] was undertaken in order to verify the following points which have been derived from the analysis and experiments described in Sections 2 and 3.

1. location of first yield point and its shift from the centre of the plate to the midpoint of the longitudinal edge as a function of b/t ratio, yield stress of steel and initial geometric imperfection
2. elastic loading and rigid-plastic unloading curves obtained from simple methods
3. ultimate strength reduction of imperfect plates due to change of mechanism

Square steel plates with varying b/t ratio, yield stress and initial imperfections were analysed in this study. A suitable finite element mesh of the quarter plate with appropriate boundary

conditions simulating those of the plate element of a box-column was used in the analysis. Quadrilateral shell elements were used in the buckling analysis and the non-linear ultimate analysis including the material and geometric effects. This produced the entire load-deflection behaviour of the plate and associated stress distributions. Bernard[4] used a quarter box-column section (angle section) instead of a plate model to model the box-columns, however, both approaches were found to give identical answers. Imperfect plates were modelled by displacing the central node by the required initial imperfection.

Buckling results agreed quite well with the simple plate buckling formula, giving a buckling coefficient K of 3.96[4]. Load-deflection curves for a b/t ratio of 50 and yield stress of 550 MPa agreed well with those obtained from the experiments as shown in Figure 7. The elastic loading and rigid-plastic unloading curves were combined to produce a continuing load-deflection curve shown as Loading/unloading curve in Figure 7. This combined curve predicted the ultimate load well, however, the lower end of the unloading curve did not agree well with that from experiments and finite element analysis.

Results for four plates with a b/t ratio of 40 ($y_0/t = 0.0$), 60 ($y_0/t = 0.4, 0.5$) and 100 ($y_0/t = 0.0$) and yield stress of 250 MPa were also used in order to study the stress distribution across these plates and to determine the first yield point. Results showed clearly that yielding commenced at the centre of plate for plates with a b/t ratio of 40 ($y_0/t = 0.0$) and 60 ($y_0/t = 0.4$) whereas for the remaining two plates, yielding commenced at the midpoint of longitudinal edges. Thus it validated the earlier results obtained using simple methods in Section 2.1, in particular the critical imperfection level of 0.5 at which the first yield point switches to the edge of the plate and thus the flip-disc mechanism. The observed reduction in ultimate strength for the steel plate with b/t ratio of 60 was only about 5% when the imperfection level was increased from 0.4 to 0.5, that is, when the type of mechanism changed from roof type to flip-disc. This does not compare well with the 15% reduction obtained from the simple elastic and rigid-plastic methods (see Figure 4), however, they all indicate that the reduction in ultimate strength due to the change of mechanism is not severe as expected.

5. Conclusions

Thin-walled steel plates with varying b/t ratio (20 to 100), yield stress (250 to 650 MPa) and initial geometric imperfection were analysed using Galerkin's method of solving Marguerre's equations to determine the change of local plastic mechanism from a roof type to a flip-disc type. This was achieved by determining the location of the first yield point in the plate. Tables and an equation that give the type of mechanism for thin plates as a function of b/t ratio, yield stress of steel and initial geometric imperfection level have been developed. Laboratory experiments on a large number of square box- and C- columns and a finite element analysis verified these results adequately. In this process Murray's hypothesis that the mechanism type was dependent on the location of first yield point has been validated.

Elastic and rigid-plastic curves were used together to predict the change of ultimate load when the type of mechanism changes. However, the observed reduction in ultimate strength due to the change of mechanism from roof to flip-disc was not as severe as that observed with stiffened plates when mechanism switched from plate to stiffener.

Local plastic mechanism tables developed from this investigation also indicate a critical or tolerance level of initial imperfection for each b/t ratio and steel grade at which the type of mechanism changes from roof to flip-disc. This can be used to determine the acceptable level of imperfection during fabrication of thin-walled steel structures considered in this investigation.

6. Acknowledgements

The author wishes to thank Professor N.W. Murray who introduced him to this interesting research topic and J. Bernard and L. Waalder who conducted some of the analytical and experimental work reported here.

7. References

1. Murray, N.W., Introduction to the Theory of Thin-walled Structures, Oxford Press, London, 1984.

2. Michelutti, W., Stiffened Plates in Combined Loading, PhD Thesis, Monash University, Melbourne, 1976

3. Murray, N.W., Recent Research into the Behaviour of Thin-walled Steel Structures, Steel Structures: Recent Research Advances and their Applications to Design, ed. M.N. Pavlovic, Elsevier Applied Science Publishers, 1985.

4. Bernard, J.P., Local Plastic Mechanisms in Thin-walled Steel Columns, BEng Thesis, Queensland University of Technology, Brisbane, 1994.

5. Mahendran, M., Box-columns with Combined Axial Compressive and Torsional Loading, PhD thesis, Monash University, Melbourne, 1985.

6. Mahendran, M. and Murray, N.W., Ultimate Load Behaviour of Box-columns under Combined Loading of Axial Compression and Torsion, Thin-walled Structures, Vol.9, 1990, pp.91-120.

7. The MacNeal-Schwendler Corporation (MSC), 1991, MSC/NASTRAN User's Manual, USA.

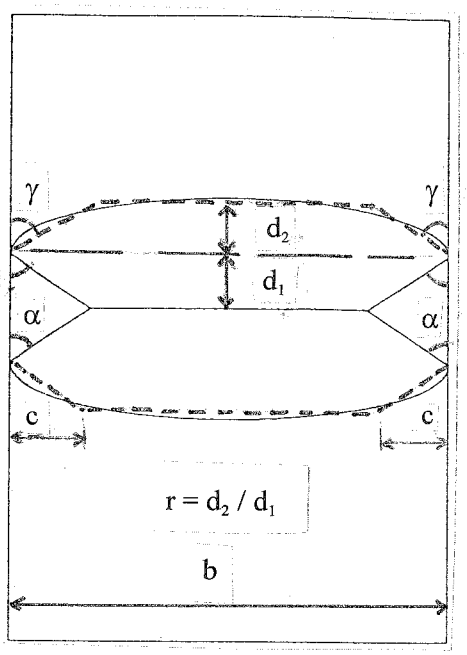

(a) Roof-shaped Mechanism

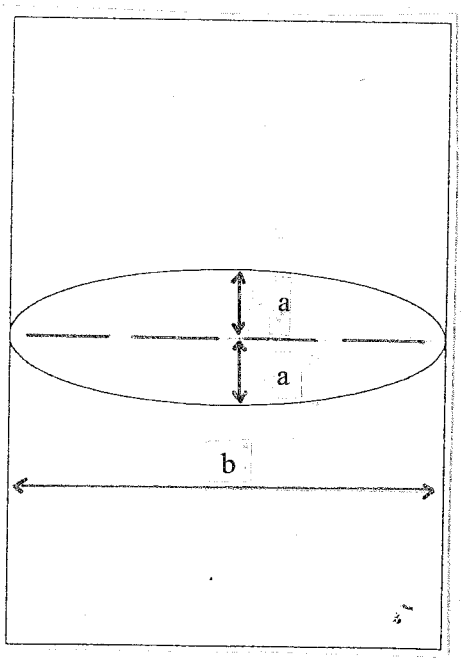

(b) Flip-disc Mechanism

Figure 1. Local Plastic Mechanisms for Thin Steel Plates under In-plane Compression

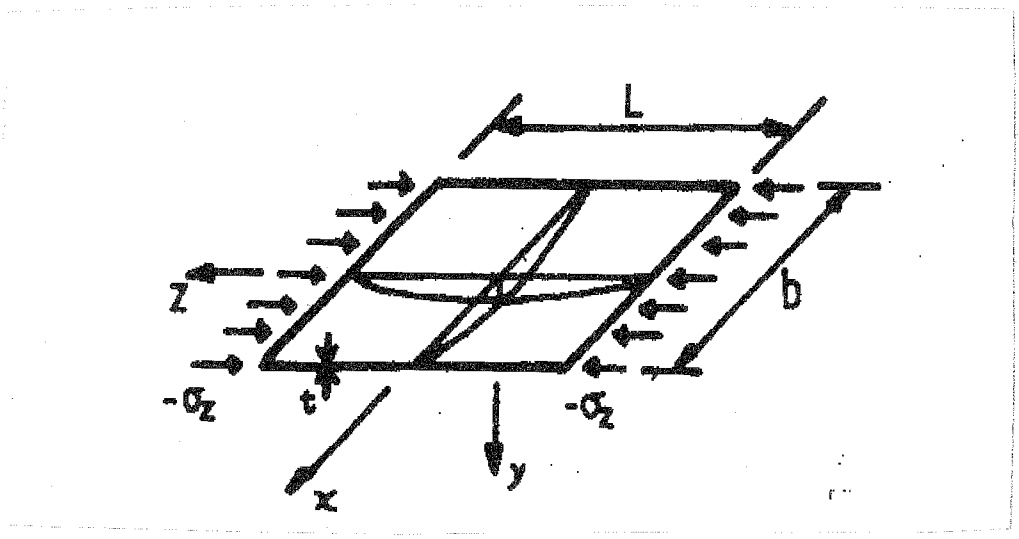

Figure 2. Imperfect Plate under In-plane Compression

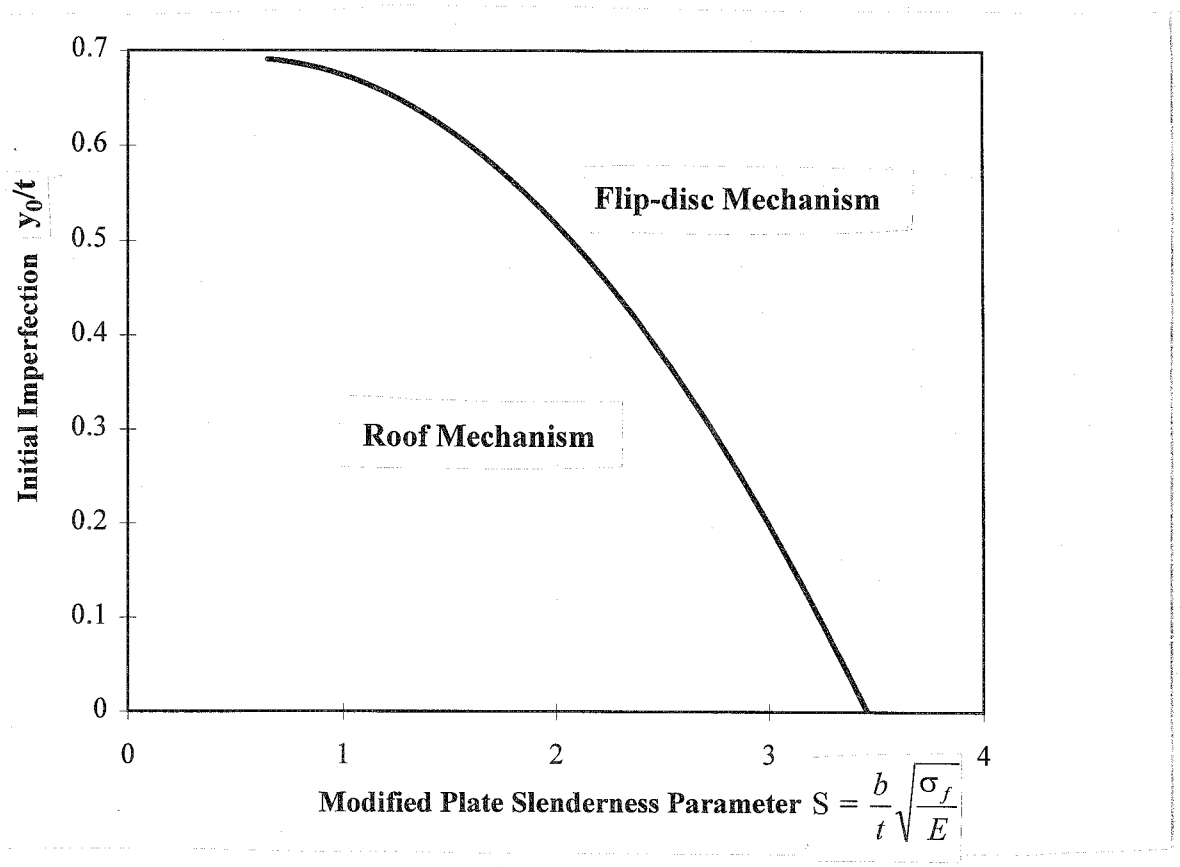

Figure 3. Effect of Modified Plate Slenderness S and Initial Imperfection y_0/t on Local Plastic Mechanisms in Thin Steel Plates

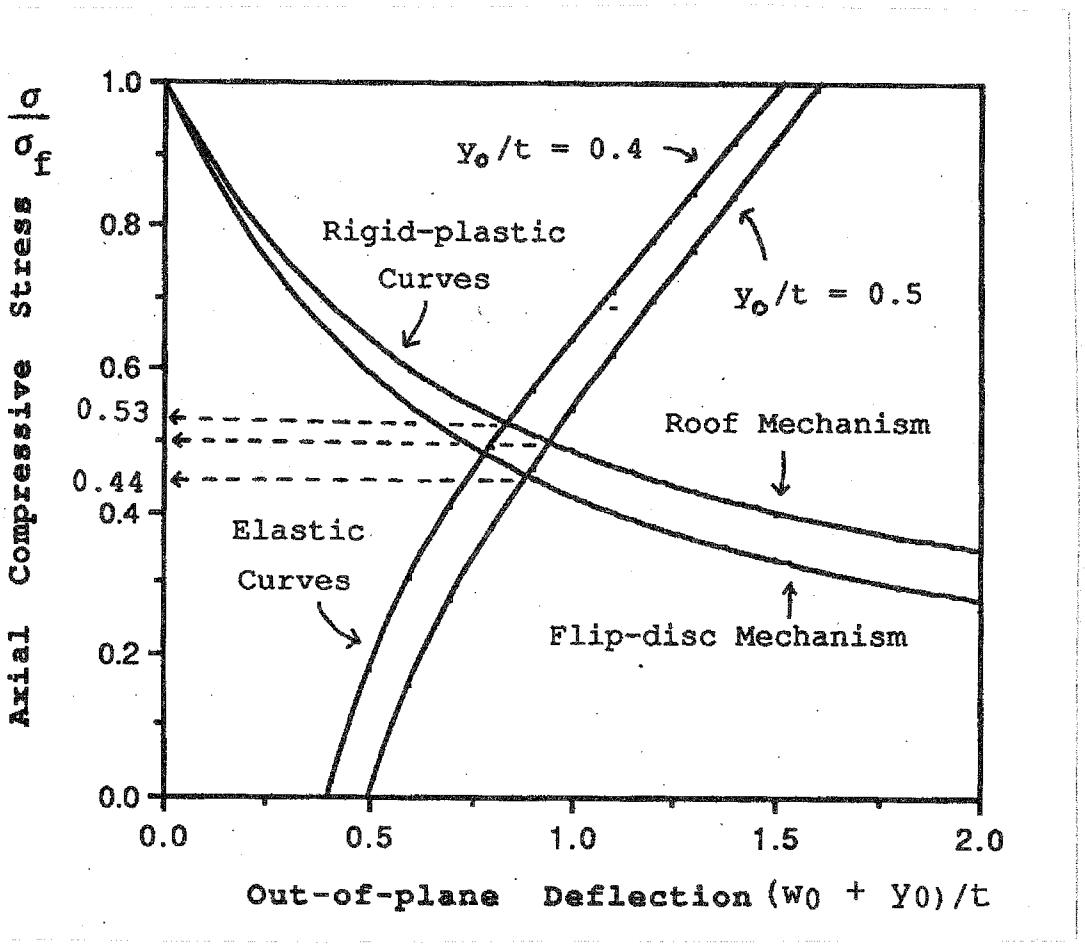

Figure 4. Elastic and Rigid-plastic Curves for Plates of b/t ratio = 60

Yield stress of steel σ_f = 250 MPa

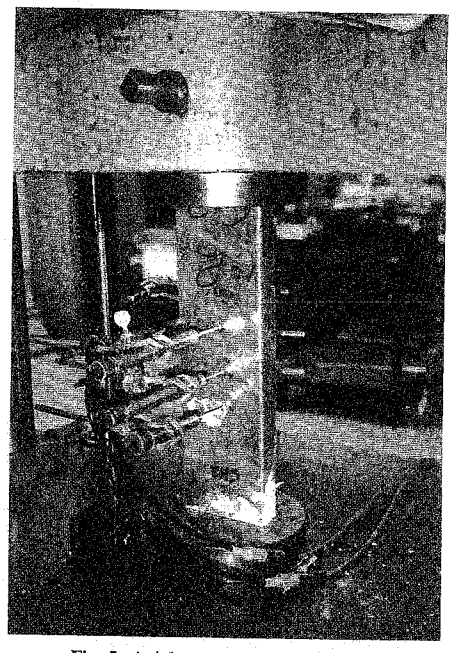

Fig. 5. Axial compression test set-up.

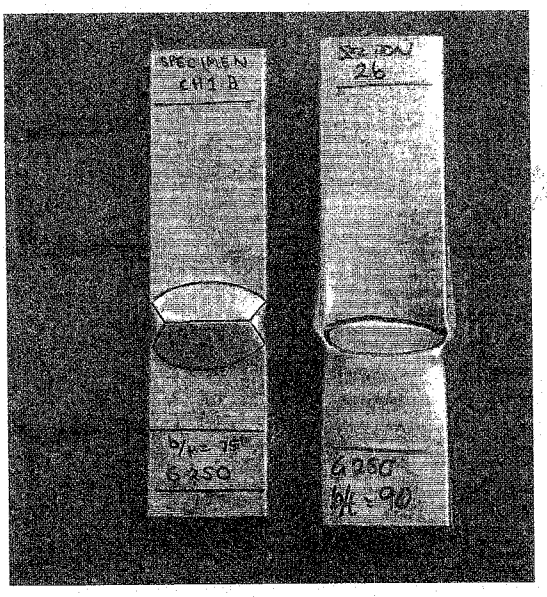

Fig. 6. Roof and flip-disc mechanisms observed during experiments. Note that the measured yield stress of Grade 250 (G250) steel was 300 MPa.

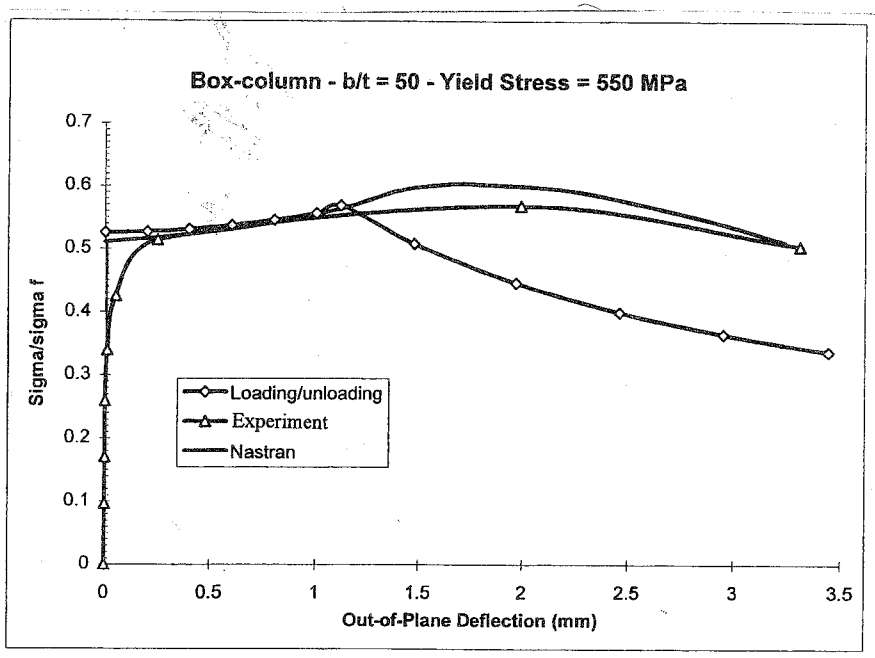

Fig. 7. Load–deflection curves for box-columns with axial compression.

Table 1 (a) Local Plastic Mechanisms for a Yield Stress of 250 MPa

b/t y_0/t	20	40	60	80	90	95	100
0.00	Roof	Roof	Roof	Roof	Roof	Roof	Flip-disc
0.03	Roof	Roof	Roof	Roof	Roof	Roof	Flip-disc
0.05	Roof	Roof	Roof	Roof	Roof	Flip-disc	Flip-disc
0.10	Roof	Roof	Roof	Roof	Roof	Flip-disc	Flip-disc
0.20	Roof	Roof	Roof	Roof	Flip-disc	Flip-disc	Flip-disc
0.30	Roof	Roof	Roof	Roof	Flip-disc	Flip-disc	Flip-disc
0.40	Roof	Roof	Roof	Flip-disc	Flip-disc	Flip-disc	Flip-disc
0.50	Roof	Roof	Flip-disc	Flip-disc	Flip-disc	Flip-disc	Flip-disc
0.60	Roof	Roof	Flip-disc	Flip-disc	Flip-disc	Flip-disc	Flip-disc
0.70	Flip-disc	Flip-disc	Flip-disc	Flip-disc	Flip-disc	Flip-disc	Flip-disc
1.00	Flip-disc	Flip-disc	Flip-disc	Flip-disc	Flip-disc	Flip-disc	Flip-disc

Table 1 (b) Local Plastic Mechanisms for a Yield Stress of 650 MPa

b/t y_0/t	20	40	50	60	70	80	90
0.00	Roof	Roof	Roof	Roof	Flip-disc	Flip-disc	Flip-disc
0.03	Roof	Roof	Roof	Flip-disc	Flip-disc	Flip-disc	Flip-disc
0.05	Roof	Roof	Roof	Flip-disc	Flip-disc	Flip-disc	Flip-disc
0.10	Roof	Roof	Roof	Flip-disc	Flip-disc	Flip-disc	Flip-disc
0.20	Roof	Roof	Roof	Flip-disc	Flip-disc	Flip-disc	Flip-disc
0.30	Roof	Roof	Flip-disc	Flip-disc	Flip-disc	Flip-disc	Flip-disc
0.40	Roof	Roof	Flip-disc	Flip-disc	Flip-disc	Flip-disc	Flip-disc
0.50	Roof	Flip-disc	Flip-disc	Flip-disc	Flip-disc	Flip-disc	Flip-disc
0.60	Roof	Flip-disc	Flip-disc	Flip-disc	Flip-disc	Flip-disc	Flip-disc
0.70	Flip-disc	Flip-disc	Flip-disc	Flip-disc	Flip-disc	Flip-disc	Flip-disc
1.00	Flip-disc	Flip-disc	Flip-disc	Flip-disc	Flip-disc	Flip-disc	Flip-disc

Table 2 (a). Local Plastic Mechanism Results for Lipped Channel Specimens

Test No.	Measured		Type of Mechanism	
	Yield Stress	b/t ratio	Analysis	Experiment
1 - 3	300	75.4, 75.7, 75.8	Roof	Roof
4, 5	300	99.4, 100.1	Flip-disc	Flip-disc
6	550	58.8	Roof	Roof
7, 8	550	59.3, 59.3	Roof	Flip-disc
9-11	550	79.4, 79.8, 79.6	Flip-disc	Flip-disc
12	600	60.0	Roof	Roof
13	600	80.2	Flip-disc	Roof
14	650	57.9	Roof	Roof
15	650	77.4	Flip-disc	Roof

Table 2 (b). Local Plastic Mechanism Results for Square Box Specimens

Test No.	Measured		Type of Mechanism	
	Yield Stress	b/t ratio	Analysis	Experiment
1a	300	42.5	Roof	Roof
2a, 3b	300	62.1, 62.5	Roof	Roof
4a	300	77.1	Roof	Flip-disc
5a, 6b	300	93.0, 93.4	Flip-disc	Flip-disc
7a	300	101.1	Flip-disc	Flip-disc
8a	550	36.4	Roof	Roof
9b	550	48.5	Roof	Flip-disc
10b, 11a	550	58.2, 61.7	Roof	Flip-disc
12b	550	67.9	Flip-disc	Flip-disc
13a	550	80.9	Flip-disc	Flip-disc
14a	600	33.3	Roof	Roof
15a	600	62.2	Roof	Roof
16a	600	81.8	Flip-disc	Flip-disc
17a	650	30.9	Roof	Roof
18a, 19b	650	50.4, 50.9	Roof	Roof
20a, 21b	650	59.9, 59.4	Roof	Roof
22a	650	59.9	Roof	Flip-disc
23a	650	78.9	Flip-disc	Flip-disc
24a, 25b	650	80.0, 80.1	Flip-disc	Flip-disc

Note. a : Box-specimens made by welding two angles
b : Box-specimens made by welding two C-sections